



2020

Anti-inflammatory effects of peptides from a marine algicolous fungus *Acremonium* sp. NTU492 in BV-2 microglial cells

Follow this and additional works at: <https://www.jfda-online.com/journal>

 Part of the [Food Science Commons](#), [Medicinal Chemistry and Pharmaceutics Commons](#), [Pharmacology Commons](#), and the [Toxicology Commons](#)



This work is licensed under a [Creative Commons Attribution-Noncommercial-No Derivative Works 4.0 License](#).

Recommended Citation

Hsiao, George; Wang, Shih-Wei; Chiang, Yin-Ru; Chi, Wei-Chiung; Kuo, Yueh-Hsiung; Phong, Do Anh; Chen, Chia-Yu; and Lee, Tzong-Huei (2020) "Anti-inflammatory effects of peptides from a marine algicolous fungus *Acremonium* sp. NTU492 in BV-2 microglial cells," *Journal of Food and Drug Analysis: Vol. 28 : Iss. 2* , Article 9.

Available at: <https://doi.org/10.38212/2224-6614.1062>

This Original Article is brought to you for free and open access by Journal of Food and Drug Analysis. It has been accepted for inclusion in Journal of Food and Drug Analysis by an authorized editor of Journal of Food and Drug Analysis.

Anti-inflammatory effects of peptides from a marine algicolous fungus *Acremonium* sp. NTU492 in BV-2 microglial cells

George Hsiao^{a,b,1}, Shih-Wei Wang^{c,d}, Yin-Ru Chiang^e, Wei-Chiung Chi^{f,1}, Yueh-Hsiung Kuo^{g,h,i}, Do Anh Phong^j, Chia-Yu Chen^k, Tzong-Huei Lee^{k,*}

^a Graduate Institute of Medical Sciences, College of Medicine, Taipei Medical University, Taipei 11031, Taiwan

^b Department of Pharmacology, School of Medicine, Taipei Medical University, Taipei 11031, Taiwan

^c Department of Medicine, Mackay Medical College, New Taipei City 25245, Taiwan

^d Graduate Institute of Natural Products, College of Pharmacy, Kaohsiung Medical University, Kaohsiung 80708, Taiwan

^e Biodiversity Research Center, Academia Sinica, Taipei 11529, Taiwan

^f Institute of Food Science, National Quemoy University, Kinmen 89250, Taiwan

^g Department of Chinese Pharmaceutical Sciences and Chinese Medicine Resources, China Medical University, Taichung 40447, Taiwan

^h Department of Biotechnology, Asia University, Taichung 41354, Taiwan

ⁱ Chinese Medical Research Center, China Medical University, Taichung 40447, Taiwan

^j International Ph.D. Program in Medicine, College of Medicine, Taipei Medical University, Taipei 11031, Taiwan

^k Institute of Fisheries Science, National Taiwan University, Taipei 10617, Taiwan

Abstract

Located in tropical and subtropical region, Taiwan is an island with high algal species diversity. In this study, a number of fungal strains were isolated from marine macroalgae collected from northeastern intertidal zone of Taiwan. Preliminary anti-inflammatory screening has shown that the methanolic extracts of solid fermented products of the red alga *Mastophora rosea*-derived fungal strain *Acremonium* sp. NTU492 exhibited significant bioactivity. In an attempt to disclose the active principles from this fungal strain, a series of separation and purification was thus undertaken, which has led to the isolation and characterization of seven compounds including four new peptides, namely acrepeptins A–D (1–4), along with previously reported destruxin B (5), guangomide A (6), and guangomide B (7). Their structures were elucidated by spectroscopic analysis and compared with literatures. Of these, acrepeptins A (1) and C (3) showed markedly inhibitory activities on nitric oxide production in lipopolysaccharide-activated microglial BV-2 cells with IC₅₀ values of 12.0 ± 2.3 and 10.6 ± 4.0 μM, respectively. Furthermore, acrepeptins A (1) and C (3) significantly attenuated the expression of inducible nitric oxide synthase in a concentration-dependent manner (5–40 μM).

Keywords: *Acremonium*, Acrepeptin, Nitric oxide, iNOS, Anti-inflammation

1. Introduction

The macroalgae growing in the intertidal zone that exists wide fluctuations of salt concentration, prolonged period of sunlight exposure, sharp variation of moisture, changing tides, abundant microorganisms, as well as lots of herbivore animals would develop strategies to adapt to arduous environment. Resembling those in higher plants, in

order to get over all the inexorable stress foisted on the macroalgae, it seemed more likely that the algae-associated fungi could exert profound effects to improve the algal ability to withstand environmental stresses [1]. Besides these, the algicolous fungi would be a promising source of biologically active secondary metabolites [2]. Although algae have been reported to be the secondary largest source of marine fungi only next to mangroves [3],

Received 5 August 2019; accepted 20 November 2019.
Available online 27 June 2020

* Corresponding author. Institute of Fisheries Science, National Taiwan University, No.1, Sec. 4, Roosevelt Rd., Taipei 10617, Taiwan.
E-mail address: thlee1@ntu.edu.tw (T.-H. Lee).

¹ Equal contribution.

<https://doi.org/10.38212/2224-6614.1062>

1021-9498/Copyright © 2020 Food and Drug Administration, Taiwan. This is an open access article under the CC BY NC ND 4.0 license (<http://creativecommons.org/licenses/by-nc-nd/4.0/>).

most of the tropical and subtropical algae have not been investigated intensively for associated microorganisms, whereas researches have been conducting in temperate zones [4]. A diverse array of novel chemical entities comprising wide spectrum of bioactivities including anticancer, antioxidant, antimycotic, antibacterial, and tyrosine kinase and elastase inhibitory activities have been isolated from algal endophytes in the recent studies [1].

Taiwan is located at tropical and subtropical region, where the macroalgae species diversity is quite high, and of the over 200 species recorded so far, 179 species have been identified [5]. Although the chemical constituents research of local macroalgae has been progressed incessantly; however, the natural products of their derived fungal strains were still rarely studied. In the preliminary screening, the methanolic extracts of solid fermented products of *Acremonium* sp. NTU492 derived from the red alga *Mastophora rosea* were found to exhibit significant anti-inflammatory activity. That prompted us to set out to search for bioactive compounds from *Acremonium* sp. NTU492, and has resulted in the isolation and identification of four new compounds 1–4 (Fig. 1) together with three known cyclic depsipeptides. This paper herein focused on the isolation and structural elucidation of the new compounds together with their anti-inflammatory activities.

2. Methods

2.1. General experimental procedures

Optical rotation was measured on a JASCO P-2000 polarimeter (Tokyo, Japan). ^1H and ^{13}C NMR were acquired on a Bruker AVIII-500 spectrometer (Ettlingen, Germany). High resolution mass spectra were obtained using a Q Exactive Plus Hybrid Quadrupole-Orbitrap Mass Spectrometer (Thermo Fisher Scientific, Bremen, Germany), respectively. IR spectra were recorded on a JASCO FT/IR 4100 spectrometer (Tokyo, Japan). Sephadex LH-20 (GE Healthcare, Uppsala, Sweden) and Diaion HP-20 (Mitsubishi Chemical, Tokyo, Japan) was used for open column chromatography. An HPLC pump L-7100 (Hitachi, Japan) equipped with a refractive index detector (Bischoff, Leonberg, Germany) was used for compound purification.

2.2. Fungal strain and culture

Acremonium sp. NTU492 was isolated from a marine alga *M. rosea* collected from the northeast coast of Taiwan, and was identified by sequencing of the

internal transcribed spacer regions of the rDNA (ITS). A BLAST search of the sequence (GenBank accession no. KY753131) led to the best match as *Acremonium* sp. The mycelium of *Acremonium* sp. NTU492 was inoculated into 500 mL flasks, each containing 50 g brown rice and 20 mL deionized water with 2% yeast extract (Becton, Dickinson and Company, Sparks, USA), 1% sodium tartrate, and 1% KH_2PO_4 . The fermentation was conducted with aeration at 25–30 °C for 10 days.

2.3. Extraction and isolation of secondary metabolites

Fermented products were lyophilized, ground into powder, and extracted three times with equal volumes of methanol. Extracts were first partitioned with *n*-hexane, and the methanol layer re-dissolved in deionized H_2O , then partitioned with ethyl acetate and concentrated to obtain dried *n*-hexane extract (2.2 g) and ethyl acetate extract (2.6 g). The ethyl acetate extract was then subjected to Sephadex LH-20 column chromatography (3.0 i.d. \times 68.0 cm), using methanol as the eluent at a flow rate of 2.3 mL/min to give 24 fractions (23.0 mL/fr.). All the fractions were combined into six portions as I–VI based on the results of TLC analysis. Portion II (#fr. 8 and 9) was further purified by a Nucleodur 100-5 C18ec column, 4.6 i.d. \times 250 mm, using 55% acetonitrile_{aq} containing 0.03% trifluoroacetic acid as eluent at a flow rate of 1 mL/min to give 1 ($R_t = 11.39$ min, 16.2 mg), 2 ($R_t = 10.89$ min, 25.8 mg), and 3 ($R_t = 15.40$ min, 19.6 mg). Portions IV (#fr. 11) was re-chromatographed on a Thermo Hypersil ODS column, 10 i.d. \times 250 mm, with 60% methanol_{aq} as eluent at a flow rate of 2 mL/min to afford 4 ($R_t = 19.90$ min, 19.1 mg), 5 ($R_t = 35.79$ min, 8.1 mg), and 6 ($R_t = 40.58$ min, 4.6 mg). Portion V (#fr. 12–15) was further purified by the same HPLC column using 55% acetonitrile_{aq} as eluent to give 7 ($R_t = 29.96$ min, 12.0 mg).

2.3.1. Acrepeptin A (1)

White powder; $[\alpha]_D^{27} -88.2$ ($c = 0.065$, MeOH); IR (ZnSe) ν_{max} : 3600–2500, 2964, 2938, 2871, 1707, 1670, 1636, 1538, 1464, 1399, 1311, and 1052 cm^{-1} ; ^1H and ^{13}C NMR data: see Tables 1 and 2; HRESIMS $[\text{M} + \text{H}]^+$ at m/z 1036.7380 (calcd. 1036.7382 for $\text{C}_{53}\text{H}_{98}\text{N}_9\text{O}_{11}$).

2.3.2. Acrepeptin B (2)

White powder; $[\alpha]_D^{27} -169.1$ ($c = 0.075$, MeOH); IR (ZnSe) ν_{max} : 3600–2500, 2931, 2876, 1715, 1670, 1627,

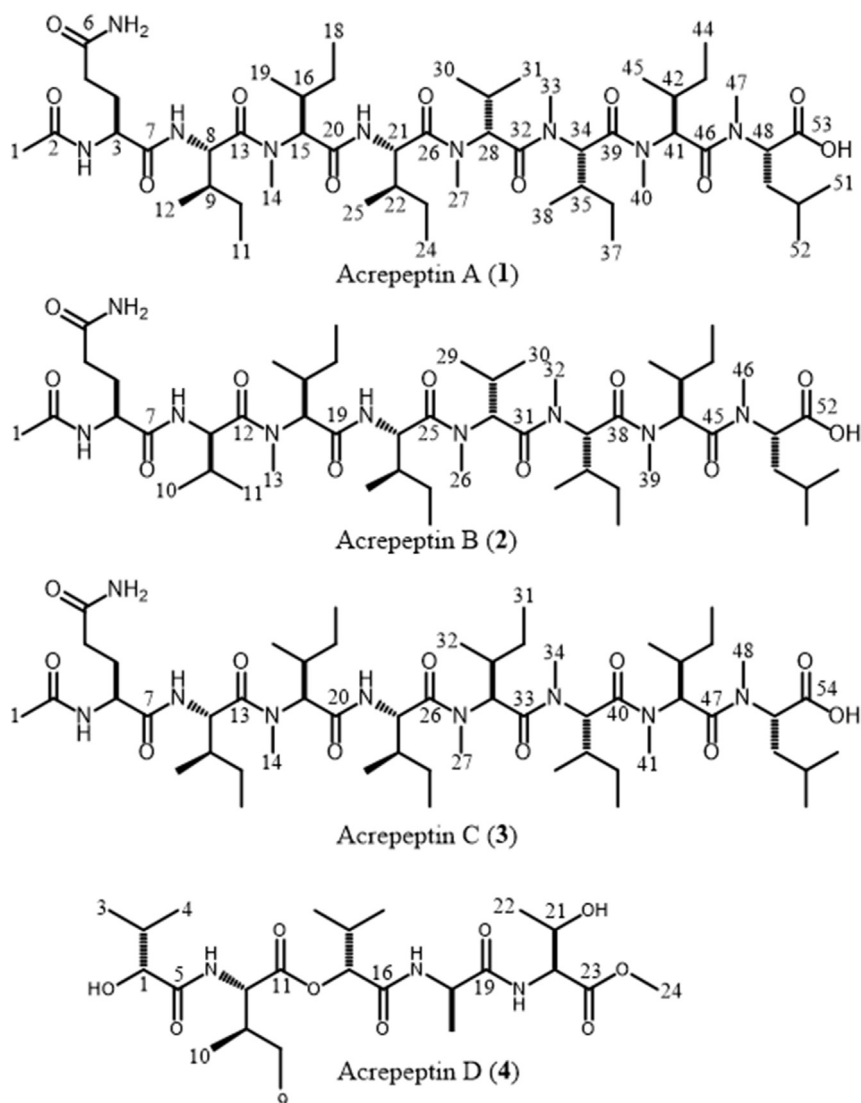


Fig. 1. Chemical structures of compounds 1–4 isolated in this study.

1541, 1464, 1403, 1289, 1131, and 1097 cm^{-1} ; ^1H and ^{13}C NMR data: see Tables 1 and 2; HRESIMS $[\text{M} + \text{H}]^+$ at m/z 1022.7243 (calcd. 1022.7224 for $\text{C}_{52}\text{H}_{96}\text{N}_9\text{O}_{11}$).

2.3.3. Acrepeptin C (3)

White powder; $[\alpha]_{\text{D}}^{27} -190.4$ ($c = 0.08$, MeOH); IR (ZnSe) ν_{max} : 3600–2500, 2965, 2874, 1711, 1675, 1627, 1539, 1459, 1405, 1308, 1282, 1205, 1131, 1098, and 1053 cm^{-1} ; ^1H and ^{13}C NMR data: see Tables 1 and 2; HRESIMS $[\text{M} + \text{H}]^+$ at m/z 1050.7544 (calcd. 1050.7537 for $\text{C}_{54}\text{H}_{100}\text{N}_9\text{O}_{11}$).

2.3.4. Acrepeptin D (4)

White powder; $[\alpha]_{\text{D}}^{27} -11.4$ ($c = 0.08$, MeOH); IR (ZnSe) ν_{max} : 3414, 2967, 2871, 1739, 1689, 1645, 1519, 1461, 1218, and 1055 cm^{-1} ; ^1H and ^{13}C NMR data:

see Tables 1 and 2; HRESIMS $[\text{M} + \text{H}]^+$ at m/z 518.3073 (calcd. 518.3072 for $\text{C}_{24}\text{H}_{44}\text{N}_3\text{O}_9$).

2.4. HPLC chiral analysis of acid hydrolysates of 1–4

The chirality of each amino acid of 1–4 was analyzed by HPLC as described previously in the literature [6]. Compounds 1–4 (each 1.5 mg) were subjected to hydrolysis with 6N HCl (0.5 mL) in a sealed tube at 110 °C for 20 h. Upon cooling, the acid in the hydrolysate was removed by Sep-Pak C₁₈ SPE column (0.5 g, Waters), and the analyte eluted by aqueous methanol was subjected to chiral analysis on a Chirex 3126 (D)-penicillamine column, 4.6 i.d. \times 250 mm, with an eluent system containing 2 mM $\text{CuSO}_{4\text{aq}}$ at a flow rate of 1 mL/min in an

Table 1. ^{13}C NMR data for compounds 1–4 (δ in ppm, mult.).

No.	1 ^{a,b}	2 ^{a,b}	3 ^{a,b}	4 ^{a,b}
1	22.6 q	22.5 q	22.5 q	71.5 d
2	169.8 s	169.7 s	169.2 s	31.4 d
3	52.1 d	52.0 d	51.8 d	16.2 q
4	28.4 t	28.3 t	28.3 t	19.1 q
5	31.8 t	31.6 t	31.6 t	173.4 s
6	174.2 s	173.7 s	173.7 s	55.4 d
7	171.8 s	171.5 s	171.5 s	36.8 d
8	52.9 d	54.1 d	52.8 d	24.6 t
9	36.4 d	30.1 d	36.2 d	11.3 q
10	24.4 t	18.8 q	24.1 t	15.3 q
11	10.5 q	17.9 q	10.9 q	171.0 s
12	15.0 q	172.0 s	14.5 q	78.0 d
13	172.6 s	30.6 q	172.2 s	30.1 d
14	30.9 q	58.9 d	30.7 q	17.0 q
15	59.2 d	32.2 d	58.9 d	18.7 q
16	32.4 d	24.0 t	32.3 d	167.9 s
17	24.2 t	10.4 q	24.0 t	47.9 d
18	10.6 q	14.9 q	10.5 q	18.2 q
19	14.9 q	169.9 s	14.8 q	172.7 s
20	170.1 s	52.7 d	169.9 s	57.8 d
21	53.0 d	35.5 d	52.6 d	66.3 d
22	35.8 d	24.1 t	35.6 d	20.1 q
23	24.3 t	10.4 q	24.2 t	171.0 s
24	10.6 q	14.6 q	10.5 q	51.9 q
25	14.7 q	172.3 s	14.7 q	
26	172.6 s	30.0 q	172.2 s	
27	30.2 q	57.3 d	30.0 q	
28	57.5 d	26.7 d	55.8 d	
29	26.9 d	18.3 q	32.7 d	
30	18.1 q	18.8q	23.5 t	
31	18.9 q	169.8 s	10.4 q	
32	170.2 s	30.0 q	14.7 q	
33	30.3 q	55.5 d	169.8 s	
34	55.8 d	32.7 d	30.1 q	
35	32.9 d	23.5 t	55.5 d	
36	23.8 t	10.5 q	32.7 d	
37	10.7 q	14.6 q	23.6 t	
38	14.8 q	170.1 s	10.3 q	
39	170.5 s	30.0 q	14.6 q	
40	30.3 q	55.2 d	170.2 s	
41	55.5 d	32.7 d	30.1 q	
42	32.9 d	23.5 t	55.2 d	
43	23.7 t	10.3 q	32.7 d	
44	11.0 q	15.0 q	23.5 t	
45	15.2 q	170.2 s	10.7 q	
46	170.4 s	31.1 q	15.0 q	
47	31.3 q	54.0 d	170.2 s	
48	54.3 d	36.5 t	31.1 q	
49	36.8 t	24.5 d	54.0 d	
50	24.8 d	20.1 q	36.5 t	
51	21.1 q	23.2 q	24.5 d	
52	23.4 q	172.7 s	20.8 q	
53	173.0 s		23.2q	
54			172.7 s	

^a Measured in DMSO- d_6 (125 MHz).

^b Multiplicities were obtained from phase-sensitive HSQC experiments.

either isocratic or gradient mode. The detector was set at UV 254 nm. All the analytical conditions and data of the hydrolysates and authentic standards were supplemented in Tables S1–S4.

2.5. Tandem mass spectrometric analysis of 1–3

The instruments used and parameters set were the same as those in our previous report [7]. All the mass spectrometric raw data were interpreted by Xcalibur. The MS/MS spectra of 1–3 were supplemented in Fig. S20–S25.

2.6. Microglial culture

The murine microglial cell line BV-2 was cultured as described in our previous reports [8]. Briefly, BV-2 cells were cultured in DMEM containing 10% fetal bovine serum (FBS), penicillin/streptomycin, L-glutamine and HEPES at 37 °C under a humidified 5% CO₂ atmosphere. Prior to the study, BV-2 cells were cultured in 0.5% FBS media, then pretreated with vehicle or the various concentrations of compound 1 or 3 for 15 min, and collected after 24 h stimulation with LPS (150 ng/mL). The conditioned medium was also collected and frozen at –80 °C.

2.7. Cell viability assays

The cellular viability of BV-2 cells with 24 h treatment of compounds 1 or 3 was assessed using the MTT test as described previously [8].

2.8. Detection of nitric oxide production

Cellular nitric oxide (NO) productions from activated BV-2 cells were evaluated by measuring the nitrite levels of NO metabolite in the conditioned medium. Their nitrite levels were determined by Griess method as previously described [9].

2.9. Western blotting

Western blot analyses were performed as previously described [10]. The quantitative supernatants of BV-2-manipulated cellular lysates were subjected to SDS-PAGE, and then transferred onto polyvinylidene fluoride membrane. These membranes were blocked with non-fat milk, washed three times, and then probed with the primary antibodies (anti-iNOS and - β -actin). After undergoing wash three times, the membranes were incubated with secondary antibodies and detected by enhanced chemiluminescence. The target protein levels were presented as the relative multiples as comparison with the control groups.

3. Results and discussion

In this study, the red alga *M. rosea* derived fungal strain *Acremonium* sp. NTU492 was cultured in solid

Table 2. ^1H NMR data for compounds 1–4 (δ in ppm, mult., J in Hz).

No.	1 ^{a,b}	2 ^{a,b}	3 ^{a,b}	4 ^{a,b}
-OH				5.51 br s
1	1.82 s	1.81 s	1.82 s	3.73 d (3.9)
2				1.97
-NH	7.97 d (8.2)	7.97 d (8.4)	7.95 d (8.2)	
3	4.25	4.27	4.27	0.76 d (6.8)
4	1.75; 1.60	1.74; 1.61	1.76; 1.61	0.90
5	2.03; 2.01	2.06; 2.03	2.08; 2.03	
-NH				7.64 d (8.5)
6				4.37 dd (8.5, 5.5)
-NH ₂	7.25 s; 6.72 s	7.22 s; 6.72 s	7.20s; 6.71 s	
7				1.87
-NH	8.13 d (8.6)	8.08 d (8.5)	8.12 d (8.7)	
8	4.48	4.43	4.48	1.20
				1.52 qd (7.2, 4.8)
9	1.75	1.95	1.76	0.86
10	1.48; 1.04	0.77	1.51; 1.05	0.88
11	0.63–0.87	0.69	0.70–0.84	
12	0.52–0.97		0.65–0.89	4.75 d (4.9)
13		3.05 s		2.01
14	3.05 s	4.78 d (11.3)	3.07 s	0.87
15	4.76 d (11.2)	1.86	4.80 d (11.1)	0.92
16	1.85	1.43; 1.17	1.87	
-NH				8.15 d (7.5)
17	1.40; 1.04	0.69–0.83	1.43; 1.05	4.44
18	0.63–0.87	0.64–0.87	0.70–0.84	1.23 d (7.2)
19	0.52–0.97		0.65–0.89	
-NH		8.28 d (7.9)		7.95 d (8.5)
20		4.47		4.26 dd (8.5, 3.3)
-NH	8.27 d (8.3)		8.28 d (8.0)	
21	4.48	1.78	4.48	4.10
-OH				5.08 br s
22	1.77	1.43; 1.06	1.79	1.04 d (6.4)
23	1.41; 1.04	0.69–0.83	1.41; 1.05	
24	0.63–0.87	0.64–0.87	0.70–0.84	3.61 s
25	0.52–0.97		0.65–0.89	
26		3.02		
27	3.01 s	5.09	3.02 s	
28	5.08 d (10.8)	2.20	5.19	
29	2.18	0.71	2.00	
30	0.67	0.78	1.14; 0.77	
31	0.77		0.70–0.84	
32		2.94 s	0.65–0.89	
33	2.92 s	5.17		
34	5.15 d (11.1)	2.00	2.95 s	
35	1.98	1.13; 0.77	5.18	
36	1.11; 0.75	0.69–0.83	2.01	
37	0.63–0.87	0.64–0.87	1.15; 0.87	
38	0.52–0.97		0.70–0.84	
39		3.02 s	0.65–0.89	
40	2.93 s	5.19		
41	5.18 d (11.0)	2.00	2.95 s	
42	1.99	1.14; 0.87	5.20	
43	1.05; 0.75	0.69–0.83	2.00	
44	0.63–0.87	0.64–0.87	1.14; 0.77	
45	0.52–0.97		0.70–0.84	
46		2.94 s	0.65–0.89	
47	2.92 s	5.03 dd (11.9, 4.2)		
48	5.00 dd (11.9, 4.0)	1.72; 1.56	2.94 s	
49	1.70; 1.55	1.21	5.04 dd (12.0, 4.1)	
50	1.19	0.83	1.73; 1.56	
51	0.76	0.78	1.23	
52	0.82		0.95	
53			0.78	

^a Measured in DMSO-*d*₆ (500 MHz).^b Signals without multiplicity were overlapped, and were obtained from HSQC or HMBC experiments.

state, and seven compounds including four new peptides 1–4 and three known compounds were obtained from the fermented products. The known compounds, destruxin B, guangomide A, and guangomide B were identified by comparison of spectroscopic data with literatures [11–13].

Compound 1, obtained as white powder, was determined to have a molecular formula of $C_{53}H_{97}N_9O_{11}$, as evidenced by its ^{13}C NMR spectrum (Table 1) and a pseudo-molecular ion $[M + H]^+$ at m/z 1036.7380 (calcd. 1036.7382 for $C_{53}H_{98}N_9O_{11}$) in the positive mode of HRESIMS analysis. The IR absorptions at 3600–2500 coupled with 1707, and 1670, 1636, 1538, and 1311 cm^{-1} revealed the presence of carboxylic acid and amide functionalities, respectively. Considering the patterns of 1H and ^{13}C NMR spectra along with its MS data, compound 1 was deduced to be a molecule comprised by amino acids with five sets of unusual *N*-methyl functionalities. The 1H NMR (DMSO- d_6 , 500 MHz) in combination of phase-sensitive HSQC spectrum of 1 revealed overlapped resonances corresponding to fifteen methyl signals at δ_H 0.52–0.97 (H₃-1, -11, -12, -18, -19, -24, -25, -30, -31, -37, -38, -44, -45, -51, and -52), five nitrogen-bearing three-proton singlets at δ_H 2.92 (H₃-33), 2.92 (H₃-47), 2.93 (H₃-40), 3.01 (H₃-27), and 3.05 (H₃-14), eight methylene signals at δ_H 1.05, 0.75 (each 1H, H₂-43), 1.11, 0.75 (each 1H, H₂-36), 1.40, 1.04 (each 1H, H₂-17), 1.41, 1.04 (each 1H, H₂-23), 1.48, 1.04 (each 1H, H₂-10), 1.70, 1.55 (each 1H, H₂-49), 1.75, 1.60 (each 1H, H₂-4), and 2.03, 2.01 (each 1H, H₂-5), eight α -methine signals at δ_H 4.25 (H-3), 4.48 (H-8), 4.48 (H-21), 4.76 (d, J = 11.2 Hz, H-15), 5.00 (dd, J = 11.9, 4.0 Hz, H-48), 5.08 (d, J = 10.8 Hz, H-28), 5.15 (d, J = 11.0 Hz, H-34), and 5.18 (d, J = 11.0 Hz, H-41), six β -methine signals at δ_H 1.75 (H-9), 1.77 (H-22), 1.85 (H-16), 1.98 (H-35), 1.99 (H-42), and 2.18 (H-29), one γ -methine signal at 1.19 (H-50), and four amine signals at δ_H 6.72 and 7.27 (each 1H, s, NH₂-Gln₁), 7.97 (1H, d, J = 8.2 Hz, NH-Gln₁), 8.13 (1H, d, J = 8.6 Hz, NH-*allo*-Ile₂), and 8.27 (1H, d, J = 8.3 Hz, NH-*allo*-Ile₄) (Table 2). The ^{13}C NMR (DMSO- d_6 , 125 MHz) coupled with phase-sensitive HSQC spectrum of 1 showed fifty-three signals including fifteen methyl carbons at δ_C 10.5 (C-11), 10.6 (C-18), 10.6 (C-24), 10.7 (C-37), 11.0 (C-44), 14.7 (C-25), 14.8 (C-38), 14.9 (C-19), 15.0 (C-12), 15.2 (C-45), 18.1 (C-30), 18.9 (C-31), 21.1 (C-51), 22.6 (C-1), and 23.4 (C-52), five *N*-methyl carbons at δ_C 30.2 (C-27), 30.3 (C-33), 30.3 (C-40), 30.9 (C-14), and 31.3 (C-47), eight methylene carbons at δ_C 23.7 (C-43), 23.8 (C-36), 24.2 (C-17), 24.3 (C-23), 24.4 (C-10), 28.4 (C-4), 31.8 (C-5), and 36.8 (C-49), eight α -methine carbons at δ_C 52.1 (C-3), 52.9 (C-8), 53.0 (C-21), 54.3 (C-48), 55.5 (C-41), 55.8 (C-34), 57.5 (C-28), and 59.2 (C-15), six β -methine carbons at δ_C 26.9 (C-

29), 32.4 (C-16), 32.9 (C-35), 32.9 (C-42), 35.8 (C-22), and 36.4 (C-9), one γ -methine carbon at δ_C 24.8 (C-50), and ten non-protonated signals at δ_C 169.8 (C-2), 170.1 (C-20), 170.2 (C-32), 170.4 (C-46), 170.5 (C-39), 171.8 (C-7), 172.6 (C-13), 172.6 (C-26), 173.0 (C-53), 174.2 (C-6) (Table 1). The COSY spectrum of 1 displayed eight sets of contiguous protons as follows: NH/H-3/H₂-4/H₂-5; NH/H-8/H-9 (H₃-12)/H₂-10/H₃-11; H-15/H-16 (H₃-19)/H₂-17/H₃-18; NH/H-21/H-22 (H₃-25)/H₂-23/H₃-24; H-28/H-29 (H₃-30)/H₃-31; H-34/H-35 (H₃-38)/H₂-36/H₃-37; H-41/H-42 (H₃-45)/H₂-43/H₃-44; H-48/H₂-49/H-50 (H₃-52)/H₃-51 (Fig. 2), which were further confirmed by the TOCSY spectrum of 1. The HMBC spectrum showed key cross-peaks of δ_H 1.82 (H₃-1)/ δ_C 169.8 (C-2); δ_H 2.03, 2.01 (H₂-5)/ δ_C 174.2 (C-6); δ_H 7.25, 6.72 (NH₂-*N*-Ac-Gln₁)/ δ_C 31.8 (C-5); δ_H 4.25 (H-3)/ δ_C 171.8 (C-7); δ_H 8.13 (NH-Ile₂)/ δ_C 171.8 (C-7); δ_H 4.48 (H-8)/ δ_C 172.6 (C-13); δ_H 3.05 (H₃-14)/ δ_C 172.6 (C-13) and 59.2 (C-15); δ_H 4.76 (H-15)/ δ_C 170.1 (C-20); δ_H 8.27 (NH-Ile₄)/ δ_C 170.1 (C-20); δ_H 4.48 (H-21)/ δ_C 172.6 (C-26); δ_H 3.01 (H₃-27)/ δ_C 172.6 (C-26) and 57.5 (C-28); δ_H 5.08 (H-28)/ δ_C 170.2 (C-32); δ_H 2.92 (H₃-33)/ δ_C 170.2 (C-32) and 55.8 (C-34); δ_H 5.15 (H-34)/ δ_C 170.5 (C-39); δ_H 2.93 (H₃-40)/ δ_C 170.5 (C-39) and 55.5 (C-41); δ_H 5.18 (H-41)/ δ_C 170.4 (C-46); δ_H 2.92 (H₃-47)/ δ_C 170.4 (C-46) and 54.3 (C-48); δ_H 5.00 (H-48)/ δ_C 173.0 (C-53) (Fig. 2), corroborating the gross structure of 1 to be *N*-acetyl-glutamine₁ → isoleucine₂ → *N*-methyl-isoleucine₃ → isoleucine₄ → *N*-methyl-valine₅ → *N*-methyl-isoleucine₆ → *N*-methyl-isoleucine₇ → *N*-methyl-leucine₈. The amino acid sequence of 1 was also confirmed by the m/z difference of the fragment ions from MS/MS spectral interpretation (Fig. 3). HPLC chiral analysis of the acid hydrolysate of 1 revealed that the absolute configurations of glutamine, isoleucine, *N*-methyl-isoleucine, *N*-methyl-valine, and *N*-methyl-leucine were *L*-, *L*-*allo*-, *L*-, *D*-, and *L*-forms, respectively. Thus, the structure of 1 was determined to be shown in Fig. 1, and it was named acrepeptin A.

The physical and NMR data of 2 and 3 were almost compatible with those of 1 except that only a structural change around their C-11 and -31 (Tables 1 and 2), respectively. The quasi-molecular ion $[M + H]^+$ at m/z 1022.7243 in the HRESIMS of 2, 14 Da less than that of 1, coupled with m/z 270.15 for the fragment of *N*-acetyl-glutamine₁ → valine₂ in the MS/MS data of 2 (Fig. 3), 14 Da less than that of 1, confirmed that the isoleucine₂ in 1 was substituted by a valine₂ in 2. The quasi-molecular ion $[M + H]^+$ at m/z 1050.7544 in the HRESIMS of 3, 14 Da more than that of 1, along with m/z 651.44 for the fragment of *N*-acetyl-glutamine₁ → isoleucine₂ → *N*-methyl-isoleucine₃ → isoleucine₄ → *N*-methyl-isoleucine₅ in the MS/MS data of 3 (Fig. 3), 14 Da more than that of

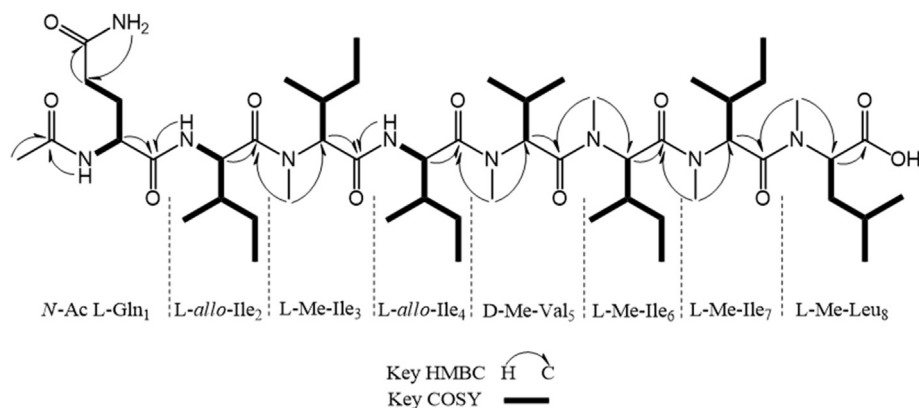


Fig. 2. Key COSY and HMBC correlations of accepeptin A (1).

1, indicated that the *N*-methyl-valine₅ in 1 was replaced by a *N*-methyl-isoleucine₅ in 3. HPLC chiral analysis of the acid hydrolysates of 2 and 3 confirmed the absolute configurations of the valine₂ in 2 and the *N*-methyl-isoleucine₅ in 3 to be *D*- and *L*-forms, respectively. Therefore, the structures of 2 and 3 were deduced to be shown.

So far, two analogues of compounds 1–3, RHM1 and RHM2, have been isolated from a sponge-derived *Acremonium* sp. [14]; however, 1–3 had different amino acid compositions and dissimilar configurations of some amino acids from those in the known analogues. Due to the presence of high proportion of unusual amino acids such as *D*-valine,

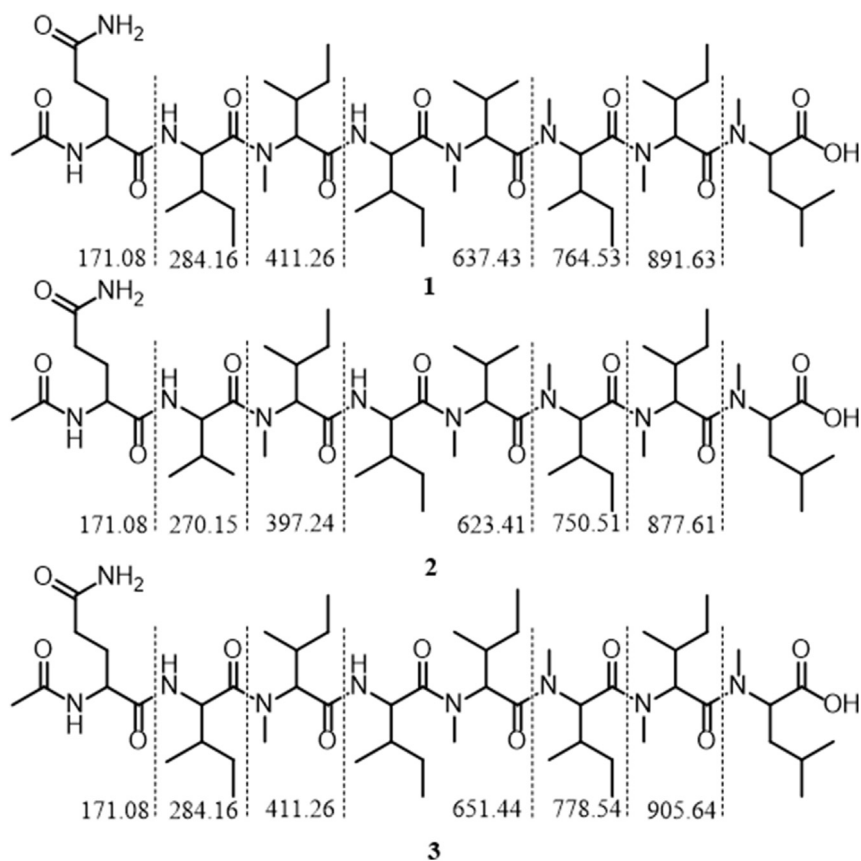


Fig. 3. The MS/MS fragments of accepeptins A–C (1–3).

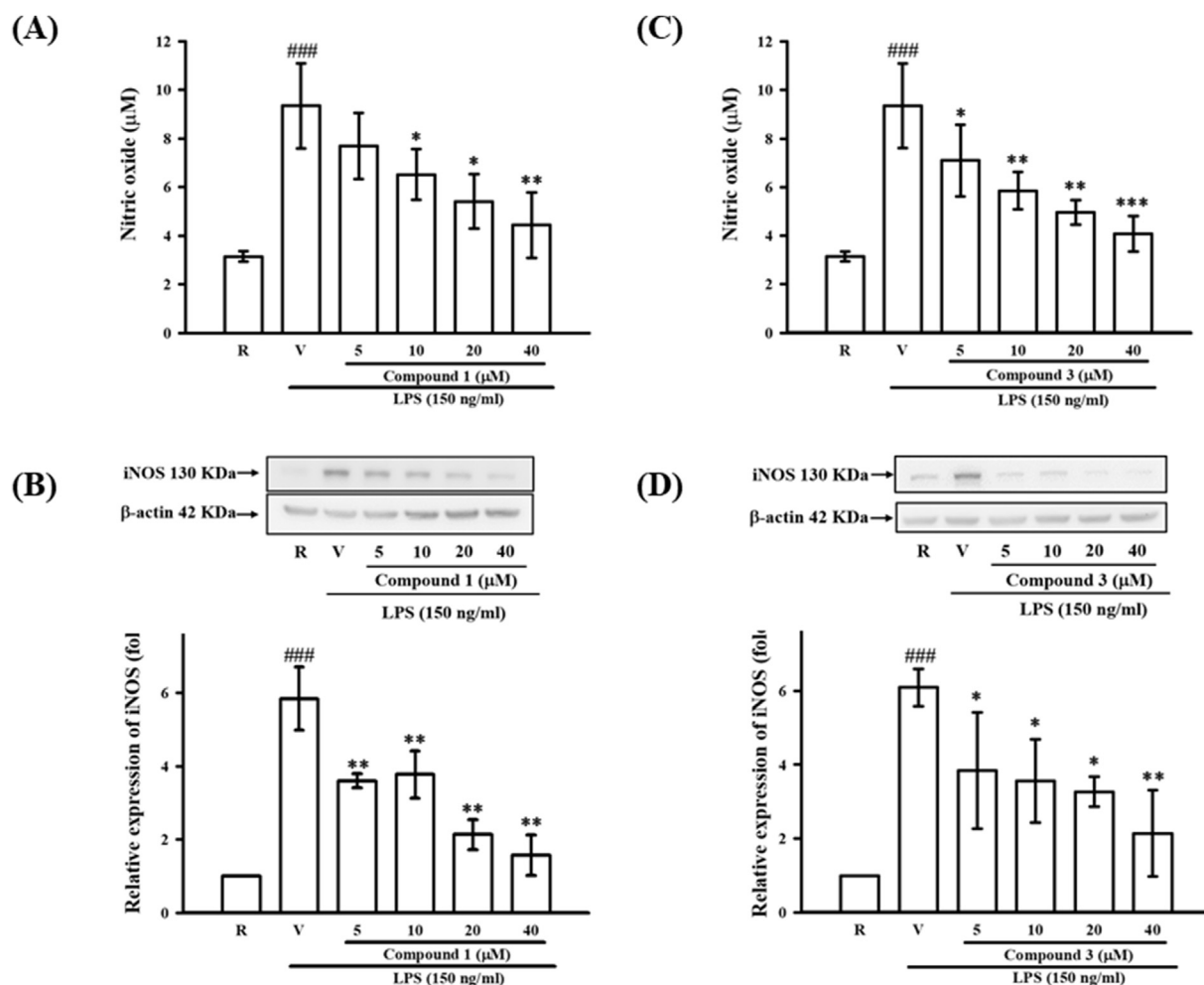


Fig. 4. Effects of compounds 1 and 3 on LPS-induced NO production (A and C) and iNOS expression (B and D) in BV-2 microglial cells. Data are expressed as the mean \pm SD ($n = 3$). ### $p < 0.001$, compared with the resting group; * $p < 0.05$ and ** $p < 0.01$, compared with the group of stimulation.

L-allo-isoleucine, *N-methyl-L-isoleucine*, *N-methyl-D-valine*, and *N-methyl-L-leucine* along with modified C- and N-termini, compounds 1–3 were likely the products of non-ribosomal peptide synthase (NRPS).

Compound 4 was assigned a molecular formula of $C_{24}H_{43}N_3O_9$ by HRESIMS and ^{13}C NMR. The IR spectrum indicated the presence of amide carbonyls (1645 and 1689 cm^{-1}), an ester carbonyl (1739 cm^{-1}), and a hydroxy and an amine (3414 cm^{-1}). Analysis of the 1H NMR (DMSO- d_6 , 500 MHz) in combination with HSQC spectrum of 4 showed four methyl signals at δ_H 0.76 (d, $J = 6.8\text{ Hz}$, H_3 -3), 1.04 (d, $J = 6.4\text{ Hz}$, H_3 -22), 1.23 (d, $J = 7.2\text{ Hz}$, H_3 -18), and 3.61 (s, H_3 -24) and five overlapped three-proton resonances at δ_H 0.86–0.92 (H_3 -4, -9, -10, -14, and -15), one

methylene signal at δ_H 1.20 and 1.52 (qd, $J = 7.2, 4.8\text{ Hz}$, H_2 -8), nine methine signals δ_H 1.87 (H-7), 1.97 (H-2), 2.01 (H-13), 3.73 (d, $J = 3.9\text{ Hz}$, H-1), 4.10 (H-21), 4.26 (dd, $J = 8.5, 3.3\text{ Hz}$, H-20), 4.37 (dd, $J = 8.6, 5.5\text{ Hz}$, H-6), 4.44 (H-17), and 4.75 (d, $J = 4.9\text{ Hz}$, H-12), three amine signals at δ_H 7.64 (d, $J = 8.3\text{ Hz}$, NH-Ile $_2$), 7.95 (d, $J = 8.5\text{ Hz}$, NH-Thr methyl ester $_5$), and 8.15 (d, $J = 7.5\text{ Hz}$, NH-Ala $_4$), and two hydroxy signals at δ_H 5.08 (br s, OH-21) and 5.51 (br s, OH-1) (Table 2). The ^{13}C NMR (DMSO- d_6 , 125 MHz) coupled with phase-sensitive HSQC spectrum of 4 showed twenty-four signals including nine methyl carbons at δ_C 11.3 (C-9), 15.3 (C-10), 16.2 (C-3), 17.0 (C-14), 18.2 (C-18), 18.7 (C-15), 19.1 (C-4), 20.1 (C-22), and 51.9 (C-24), one methylene carbon at δ_C 24.6 (C-8), nine methine carbons at δ_C 30.1 (C-13), 31.4 (C-2), 36.8 (C-7), 47.9

(C-17), 55.4 (C-6), 57.8 (C-20), 66.3 (C-21), 71.5 (C-1), and 78.0 (C-12), and five non-protonated carbons at δ_C 167.9 (C-16), 171.0 (C-23), 171.0 (C-11), 172.7 (C-19), and 173.4 (C-5). Analysis of COSY spectral data of **4** allowed the assignments of three spin systems as follows: OH-1/H-1/H-2 (H₃-3)/(H₃-4); NH/H-6; H-7/H₃-10; H₂-8/H₃-9; H-12/H-13 (H₃-14)/H₃-15; NH/H-17/H₃-18; NH/H-20; H₃-22/H-21/OH-21. In the HMBC spectrum of **4**, key correlations including δ_H 3.73 (H-1)/ δ_C 173.4 (C-5); δ_H 7.64 (NH-Ile₂)/ δ_C 173.4 (C-5); δ_H 4.37 (H-6)/ δ_C 36.8 (C-7); δ_H 1.20, 1.52 (H₂-8)/ δ_C 36.8 (C-7); δ_H 4.37 (H-6)/ δ_C 171.0 (C-11); δ_H 4.75 (H-12)/ δ_C 171.0 (C-11) and 167.9 (C-16); δ_H 4.44 (H-17)/ δ_C 167.9 (C-16) and 172.7 (C-19); δ_H 7.95 (NH-Thr methyl ester₅)/ δ_C 172.7 (C-19); δ_H 4.26 (H-20)/ δ_C 66.3 (C-21) and 171.0 (C-23); δ_H 3.61 (H₃-24)/ δ_C 171.0 (C-23) established the structure of each amino acid and their connectivity to be 2-hydroxy-3-methylbutanoic acid₁ → isoleucine₂ → 2-hydroxy-3-methylbutanoic acid₃ → alanine₄ → threonine methyl ester₅. HPLC chiral analysis of the acid hydrolysate of **4** indicated that the absolute configurations of 2-hydroxy-3-methylbutanoic acid, isoleucine, alanine, and threonine methyl ester were *R*-, *L*-*allo*-, *D*-, and *L*-forms, respectively. Accordingly, the structure of **4** was determined to be a linear pentapeptide as shown.

All seven compounds were subjected to nitric oxide production inhibitory activity assays. Of the compounds tested, acpeptins **A** (**1**) and **C** (**3**) showed moderate inhibitory activities on NO production in LPS-activated microglial BV-2 cells with IC₅₀ values of 12.0 ± 2.3 and 10.6 ± 4.0 μM, respectively (Fig. 4A and C). Curcumin was used as a positive control with an IC₅₀ value of 6.0 ± 0.3 μM (*n* = 3). The cellular viabilities of **1** and **3** (20 μM) was 86 ± 2% and 82 ± 6%, respectively. Furthermore, it was also found that compounds **1** and **3** concentration-dependently inhibited microglial iNOS expression stimulated by LPS (Fig. 4B and D). It was speculated that the *L*-*allo*-isoleucine₂ in **1** and **3** instead of *D*-valine₂ in **2** could play a crucial role in the anti-inflammatory activity.

Acknowledgments

This work was supported by a grant from the Ministry of Science and Technology (MOST 107-

2320-B-002-017-MY3) of Taiwan to T.-H. Lee. We thank Ms. S.-L. Huang and Ms. S.-Y. Sun, Instrumentation Center of the College of Science, National Taiwan University for the NMR and MS data acquisition, respectively.

Appendix A. Supplementary data

Supplementary data to this article can be found online at <https://doi.org/10.38212/2224-6614.1062>.

References

- [1] Sarasan M, Puthumana J, Job N, Han J, Lee JS, Philip R. Marine algiculous endophytic fungi – a promising drug resource of the era. *J Microbiol Biotechnol* 2017;27:1039–52.
- [2] Schulz B, Boyle C, Draeger S, Römmert AK, Krohn K. Endophytic fungi: a source of novel biologically active secondary metabolites. *Mycol Res* 2002;106:996–1004.
- [3] Jones EBG. Marine fungi: some factors influencing biodiversity. *Fungal Divers* 2000;4:53–73.
- [4] Jones EBG, Stanley SJ, Pinruan U. Marine endophyte sources of new chemical natural products: a review. *Bot Mar* 2008;51:163–70.
- [5] Huang SF. Seaweeds of northeastern Taiwan. Taipei: National Taiwan Museum; 2000.
- [6] Bisel P, Schlauch M, Weckert E, Sin K, Frahm A. Expeditionary synthesis and chromatographic resolution of (+)- and (-)-*trans*-1-benzylcyclohexan-1,2-diamine hydrochlorides. *Chirality* 2001;13:89–93.
- [7] Lee MS, Yang YL, Wu CY, Chen YL, Lee CK, Tzean SS, et al. Efficient identification of fungal antimicrobial principles by tandem MS and NMR database. *J Food Drug Anal* 2019;27:860–8.
- [8] Hsiao G, Chi WC, Pang KL, Chen JJ, Kuo YH, Wang YK, et al. Hirsutane-type sesquiterpenes with inhibitory activity of microglial nitric oxide production from the red alga-derived fungus *Chondrostereum* sp. NTOU4196. *J Nat Prod* 2017;80:1615–22.
- [9] Wang S, Suh JH, Hung WL, Zheng X, Wang Y, Ho CT. Use of UHPLC-TripleQ with synthetic standards to profile anti-inflammatory hydroxycinnamic acid amides in root barks and leaves of *Lycium barbarum*. *J Food Drug Anal* 2018;26:572–82.
- [10] Chang JC, Hsiao G, Lin RK, Kuo YH, Ju YM, Lee TH. Bioactive constituents from the termite nest-derived medicinal fungus *Xylaria nigripes*. *J Nat Prod* 2017;80:38–44.
- [11] Sato H, Yoshida M, Murase H, Nakagawa H, Doi T. Combinatorial solid-phase synthesis and biological evaluation of cyclodepsipeptide destruxin B as a negative regulator for osteoclast morphology. *ACS Comb Sci* 2016;18:590–95.
- [12] Sy-Cordero AA, Graf TN, Adcock AF, Kroll DJ, Shen Q, Swanson SM, et al. Cyclodepsipeptides, sesquiterpenoids, and other cytotoxic metabolites from the filamentous fungus *Trichothecium* sp. (MSX51320). *J Nat Prod* 2011;74:2137–42.
- [13] Amagata T, Morinaka BI, Amagata A, Tenney K, Valeriote FA, Lobkovsky E, et al. *J Nat Prod* 2006;69:1560–65.
- [14] Boot CM, Tenney K, Valeriote FA, Crews P. Highly *N*-methylated linear peptides produced by an atypical sponge-derived *Acremonium* sp. *J Nat Prod* 2006;69:83–92.